Plant Soil (2018) 430:219–231
https://doi.org/10.1007/s11104-018-3707-5

Cadmium reduces zinc uptake but enhances its translocation in the cadmium-accumulator, *Carpobrotus rossii*, without affecting speciation

Miaomiao Cheng[1] • Peter M. Kopittke[2] • Anan Wang[1] • Peter W.G. Sale[1] • Caixian Tang[1*]

[1] Department of Animal, Plant and Soil Sciences, Centre for AgriBioscience, La Trobe University, Victoria, 3086, Australia
[2] School of Agriculture and Food Sciences, The University of Queensland, St. Lucia, Queensland, 4072, Australia

Abstract

Background and aims: Interactions between Cd and Zn occur in soils and plants but are inconsistent. This study examined how Cd/Zn interactions influence the growth of *Carpobrotus rossii* (Haw.) and the accumulation of Cd and Zn in plants.
Methods: Plants were grown in nutrient solutions containing 5-100 μM Zn and 0, 5 or 15 μM Cd. Plant growth and tissue concentrations were measured, and the speciation of Zn within the plant tissues determined using synchrotron-based X-ray absorption spectroscopy.
Results: There was an additive negative interaction between Cd and Zn on root growth. Only the highest level of Zn (100 μM) decreased Cd concentrations in root and shoot tissues (by 40-64%), whilst 100 μM Zn enhanced Cd translocation at 5 μM Cd but decreased it at 15 μM Cd. In contrast, both 5 and 15 μM Cd decreased Zn concentrations in root and shoot tissues but increased Zn translocation by 30-90%. This interaction was not associated with changes in Zn speciation within the plants, with most Zn associated with oxalate (48-87%).
Conclusions: The presence of Zn and Cd resulted in an additive negative effect on root growth, but an antagonistic pattern in their accumulation in shoots of *C. rossii*.

Key words: Cd/Zn interaction, phytoremediation, synchrotron, XANES, Zn speciation, Zn translocation

Introduction

Cadmium (Cd) is considered to be one of the most environmentally toxic pollutants, accumulating in plant tissues to levels that are harmful in the diets of animals and humans without being toxic to the plant itself. It is known that Cd enters the environment as a result of the application to soil of a range of materials, including sewage sludge used as soil amendments, phosphate fertilizers, waste from incinerators, and other industrial products (Nicholson *et al.*, 1994). Among the various approaches used for remediation, phytoextraction is considered to be a cost-effective and environmentally friendly way to remove Cd from contaminated soils (Mahar *et al.*, 2016).

Zinc (Zn) is an essential micronutrient for plants but can also be toxic at elevated concentrations. Both Cd and Zn have similar geochemical and environmental properties, and are often co-located in soils, with this often resulting in Cd and Zn interacting with each other in soils and plants (Li *et al.*, 2009). However, the nature of these interactions are difficult to predict, as they can be either antagonistic or synergistic, while other times there is no interaction. It has been demonstrated that the interaction between Zn and Cd depended upon plant ecotype, metal type, external metal concentration and cultural method (Benáková *et al.*, 2017; Cojocaru *et al.*, 2016; Qiu *et al.*, 2011; Li *et al*., 2009; Lombi *et al*., 2001). Indeed, Li *et al.* (2009) reported that the addition of 500 µM Zn increased shoot Cd accumulation in the Cd/Zn hyperaccumulating ecotype of *Sedum alfredii* but decreased it in the non-hyperaccumulating ecotype, while the addition of 100 µM Cd did not influence Zn accumulation in either ecotype. In contrast, for *Potentilla griffithii*, another Cd/Zn hyperaccumulator, the addition of 2.5 mM Zn to the nutrient solution decreased Cd accumulation in roots but increased it in shoots, while 0.2 and 0.4 mM Cd increased accumulation of Zn in the roots but decreased its accumulation in the shoots (Qiu *et al.*, 2011). Furthermore, the addition of 10 µM Zn decreased Cd uptake by both ecotypes of Cd/Zn hyperaccumulator *Noccaea (Thlaspi) caerulescens* at 0.2 µM Cd, while it only caused a 35% decrease in the Prayon ecotype but not in the Ganges ecotype at 10 µM Cd (Lombi *et al*., 2001). In a similar manner, a range of interactions have been observed in three oilseed rape (*Brassica napus*) cultivars, where 10 µM Zn decreased Cd concentrations in the shoot tissue of cv. Navajo while 5 µM Cd decreased Zn concentrations in root tissues of all three cultivars (Benáková *et al.*, 2017). In contrast, for *B. napus*, when compared to treatments containing Cd or Zn alone, tissue concentrations of both Cd and Zn decreased when grown in soils enriched with a mixture of both Cd and Zn (Cojocaru *et al.*, 2016). Therefore, in order to broaden the use of phytoremediation in Cd/Zn contaminated environments, it is important to understand the mechanisms of the Cd and Zn interactions, particularly from a species-specific perspective.

Carpobrotus rossii is a Cd accumulator and is tolerant to high levels of Zn and salinity (Zhang *et al.*, 2014), and is thus a good species for studying the interactions between Zn and Cd. A previous soil-based study using *C. rossii* showed that compared to the treatments containing either Cd or Zn alone, the combination of Zn and Cd significantly increased the Cd content in the shoots but decreased the Zn content in the shoots, with an inconsistent effect on Cd and Zn translocation (Zhang et al., 2014). In this previous study, the Zn-induced increase in the shoot Cd content was partly attributed to the increased concentration of Cd in the rhizosphere (Zhang *et al*., 2014). However, overall, it remains unclear whether changes in the Cd and Zn contents of plant tissues are primarily due to interactions within soils or if they are due to interactions within the plant itself. For example, apart from influencing soil availability, the addition of Cd/Zn may also influence translocation by altering their speciation in plant tissues. It has been reported that Zn forms complexes with phytic acid, histidine, and phosphate in plant roots, and is then transported as the free Zn^{2+} ion or as Zn-organic complexes within the xylem sap (Kopittke *et al.*, 2011b, Monsant *et al.*, 2011). Of particular interest, it was shown for *C. rossii* that the addition of Cd decreased tissue concentrations of organic acids but increased P concentrations, with these changes potentially influencing the translocation and accumulation of Zn (Cheng *et al*., 2018). However, there is little information on the mutual effects of Cd and Zn on their translocation and accumulation within the

tissues of *C. rossii*. This is needed in order to understand how metals accumulate in *C. rossii* when grown in Cd/Zn contaminated environments.

The present study aimed to examine the effect of Cd and Zn on the growth of *C. rossii* and Cd/Zn interactions on the speciation, translocation and accumulation of both Cd and Zn. It was hypothesized that Cd and Zn would have synergistic effects on the growth of *C. rossii*, but have antagonistic effects on their translocation and accumulation due to the competition between them within the plant. Synchrotron-based X-ray absorption spectroscopy (XAS) was used for the *in situ* analyses of Zn speciation in hydrated (frozen) plant tissues. The results of this study provide an understanding of how Cd and Zn affect the accumulation of each other within the plant, and will assist in improving the efficiency of phytoremediation for Cd and Zn co-contaminated soils.

Materials and methods

Plant growth

Uniform cuttings of *Carpobrotus rossii* (Haw.) Schwantes (Aizoaceae) were cut from the mother plant, washed with tap water, and transplanted to polyethylene pots (5 L) filled with a basal nutrient solution (Cheng *et al.*, 2018). The nutrient solution was prepared using deionized water and had the following composition (μM): 200 $MgSO_4$; 10 KH_2PO_4; 600 K_2SO_4; 600 $Ca(NO_3)_2$; 20 FeNaEDTA; 5 H_3BO_3; 1 $MnSO_4$; 0.2 $CuSO_4$; 0.03 Na_2MoO_4; 1 $ZnSO_4$. Such a nutrient composition was shown to be adequate for the optimal growth of *C. rossii*. The solutions were continuously aerated during plant growth and replaced every 6 d. The plants were grown in a controlled environment growth room with a day/night temperature regime of 20/18 °C, a relative humidity of 50%, and a photoperiod of 14 h with a light intensity of 400 μmol m^{-2} s^{-1}. The plant roots were well developed after two weeks and three uniform rooted cuttings were chosen and transferred to new pots containing the treatment solutions. The experiment consisted of three Cd concentrations (0, 5 and 15 μM) and three Zn concentrations (5, 30 and 100 μM) in three replicates. Cadmium and Zn were added as $Cd(NO_3)_2$ and $Zn(NO_3)_2$, respectively because NO_3^- has a minimal effect on the speciation of Cd and Zn in solutions. The nutrient solutions were renewed every 3 d, and solution pH was buffered using 2 mM MES [2-(N-morpholino) ethanesulphonic acid] and adjusted daily to ca. 6.0 with 1 M KOH. Plants were harvested after growth for 10 d in the treatment solutions.

Plant harvest and analysis

Plants were separated into shoots and roots, and fresh weights recorded. After washing with deionized water, the shoots were divided into three parts, with one frozen in liquid nitrogen and stored at -80 °C, one frozen in liquid nitrogen and then freeze-dried and the third oven-dried at 80 °C in paper bags. Similarly, roots were divided into three parts, with first two parts being immersed in ice-cold 20 mM $Ca(NO_3)_2$ for 15 min, washed with deionized water, frozen in liquid nitrogen and then either stored at -80 °C or freeze-dried, while the third part was immersed in ice-cold 20 mM Na_2-EDTA for 15 min to remove Cd and/or Zn adhering to the root surface and then washed with deionized water and oven-dried at 80 °C. The morphological parameters (length, average diameter and surface area) of the roots were determined using a root scanner at 600 dpi (Epson Perfection 4990 Scanner, model J131B, Epson Inc.) before being oven-dried for chemical analysis. Given that plant growth was exponential during the treatment period, the relative growth rate (RGR) was calculated according to the equation $RGR = (\ln W_2 - \ln W_1)/(t_2 - t_1)$, where W_1 and W_2 were the dry matter weight of the entire plant at the beginning and the end of the treatment period, and $(t_2 - t_1)$ was the treatment duration (Hunt, 2012). In addition, the specific uptake was calculated by dividing total amount of Cd (or Zn) in the plants by total root length.

The oven-dried samples were ground and digested using concentrated HNO_3 in a microwave digester (Multiwave 3000, Anton Paar), and the concentrations of various elements in the digests analyzed using an inductively coupled plasma optical emission spectrometry (ICP-OES) (Perkin Elmer Optima 8000, MA, USA).

Zinc speciation by X-ray absorption spectroscopy (XAS)
Zinc K-edge X-ray absorption near edge structure (XANES) spectra were collected at the XAS Beamline at the Australian Synchrotron, Melbourne, as described by Kopittke et al. (2011b). The energy of each spectra was calibrated by simultaneous measurement in transmission mode of a metallic Zn foil reference. The spectra were collected in fluorescence mode using a 100-element solid-state Ge detector. To minimize beam-induced artifacts and thermal disorder, samples were placed in a cryostat sample holder (maintained at ca. 12 K, liquid helium). The beam size was adjusted to approximately 0.5 × 1 mm.

For the plant tissues, XAS analyses were conducted only for the five treatments containing either 5 or 100 μM Zn (i.e. not for any of the three treatments containing 30 μM Zn). For freeze-dried samples, the tissues were ground to a fine powder at room temperature before being placed into a sample holder with Kapton tape windows and transferred to the cryostat for analysis. For hydrated (frozen) samples, 1-2 g of the plant tissues were placed in an agate mortar and pestle cooled using liquid nitrogen, before being ground to a fine powder whilst keeping under liquid nitrogen. The well-homogenized samples were then placed into a sample holder with Kapton tape windows cooled with liquid nitrogen, and transferred to the cryostat for analysis. For these hydrated samples, tissues were not thawed at any point between harvest and analysis.

In addition to plant tissues, we also examined a total of eleven Zn standards, including seven aqueous compounds and four finely ground powders. The seven aqueous standards consisted of solutions with the following final concentrations (i) 4 mM $Zn(NO_3)_2$, and (ii-vii) 4 mM $Zn(NO_3)_2$ mixed with 20 mM cysteine, citric acid, histidine, phytic acid, oxalic acid, or 0.5% polygalacturonic acid. These seven aqueous standards were prepared using 40 mM stock solutions of $Zn(NO_3)_2$ together with 200 mM cysteine, citric acid, histidine, phytic acid, oxalic acid, or 1% polygalacturonic acid. All aqueous standards (other than polygalacturonic acid) were mixed in 30 % glycerol to limit ice-crystal formation during cooling, and adjusted to pH ca. 6 using 0.1 M NaOH [except for the 4 mM $Zn(NO_3)_2$]. Where constants were available, GEOCHEM-EZ was used to model the standard solutions of Zn-citrate, Zn-oxalate, Zn- histidine, and Zn-cysteine, indicating that >99% of Zn was complexed with citric acid, >99% with oxalic acid, 99% with histidine, and >96% with cysteine. In addition to the seven aqueous standards, we also prepared four solid standards, being ZnO (Sigma Aldrich, 93632), $Zn_3(PO_4)_2$ (Sigma Aldrich,587583), $[ZnCO_3]_2 \cdot [Zn(OH)_2]_3$ (Sigma Aldrich, 96466), and $ZnCO_3 \cdot 2ZnO \cdot 3H_2O$ (Ajax, 1518). These four solids were diluted to a Zn concentration of 100 mg kg^{-1} using cellulose.

Once the samples or standards had been prepared and placed into the cryostat, we collected the XANES spectra. When doing these XANES scans, we first compared spectra from hydrated plant tissues with those from freeze-dried tissues in order to allow an assessment of potential changes in speciation resulting from the freeze-drying process. This is because freeze-dried tissues are commonly used, due to their higher tissue concentrations (on a mass basis) and because they are easier to handle. However, it was found that freeze-drying resulted in a slight change in the XANES spectra (see later discussion), and thus hereafter, all samples examined were hydrated (frozen) unless otherwise stated. Next, we examined whether the XANES analyses themselves caused beam damage during scanning. For this, we did three consecutive scans at the same physical location on a plant tissue sample. For the first, we did a quick XANES scan (same number of energy steps, but with 10-times shorter dwell per energy), followed by a normal XANES scan, which was followed again by a quick XANES scan. We then compared these three scans to see if they differed, but no differences were observed, indicating that there was no observable sample damage during analysis. Finally, once we had established the correct operating procedure (i.e. using hydrated samples, with these not damaged by the XANES analyses), we then analyzed the tissue samples from the five treatments plus the eleven standards. Multiple XANES scans were performed for each sample, with

two scans per standard, and either two or three scans for each plant tissue sample. For these scans, the position was moved to different areas of the sample after each scan.

The XANES spectrum for each scan was energy-normalized using the reference energy of the Cd foil, with replicate spectra for each sample merged using Athena (version 0.9.22) (Ravel and Newville, 2005). The linear combination fitting (LCF) was performed using Athena to identify the relative proportions of standard spectra within the sample spectra. The fitting energy range was –20 to +30 eV relative to the Zn K-edge, and a maximum of two standards were permitted for each fit.

Statistical analysis
Treatment differences were tested for significance ($P \leq 0.05$) by Duncan's multiple range test following a two-way analysis of variance performed with GenStat v.11 (VSN international).

Results
Plant growth
Increasing solution concentrations of Cd decreased root weight by up to 37% while Zn decreased root weight by up to 52% (Figure 1a). However, a significant Zn × Cd interaction was observed (P<0.01, Table 1), with the magnitude of the decrease in root weight upon addition of Cd being greater at 100 µM Zn than at 5 or 30 µM Zn, and greater at 15 µM Cd than at 5 µM Cd (Figure 1a). For example, the addition of 5 µM Cd did not influence root weight, while 15 µM Cd decreased the root weight by 26% at 30 µM Zn and by 71% at 100 µM Zn.

In contrast to the effect on root weight, the concentrations of Zn and Cd in the nutrient solutions had comparatively little impact on shoot weight (Figure 1b). The interaction between Zn and Cd was found to be significant (P <0.05, Table 1). Specifically, there were no differences in the shoot weight between the 5 and 15 µM Cd treatments, irrespective of the Zn level, while increasing solution Zn from 30 to 100 µM decreased shoot weight by 25% at 0 µM Cd. Furthermore, increasing the Cd concentration from 0 to 15 µM decreased shoot weight by 25% at 30 µM Zn but did not affect it at 5 or 100 µM Zn.

Not only did the concentration of Cd and Zn influence root and shoot weight, but it also influenced RGR. A highly significant Zn × Cd interaction was observed for RGR (P<0.001, Table 1), with the magnitude of adverse impact of Cd depending upon the Zn concentration in nutrient solution. The addition of Cd did not influence RGR at 5 µM Zn but decreased RGR by 25-45% at 30 µM Zn. In contrast, the addition of 5 µM Cd, but not 15 µM Cd, increased the RGR at 100 µM Zn

Root traits
Increasing solution concentrations of Cd or Zn decreased root length by up to 75% (P<0.001, Table 1 and Figure 2a). However, a highly significant Zn × Cd interaction was observed (P<0.001, Table 1). Specifically, at 5 and 100 µM Zn, the magnitude of reduction in root length was greater with the addition of 15 µM Cd (58-63%) than of 5 µM Cd (22-40%), whereas the opposite was found at 30 µM Zn, with greater reduction at 5 µM Cd (54%) than at 15 µM Cd (35%). Similar trends were observed for root surface area although the magnitude of decrease with increasing concentrations of Cd and Zn was smaller than for root length (Figure 2b). Overall, increasing concentrations of Zn to 100 µM or concentrations of Cd to 15 µM increased root diameter by 23-30% (Figure 2c), with no significant Cd × Zn interaction (Table 1).

Plant uptake and tissue Cd concentration
As expected, increasing solution Cd concentration increased the concentrations of Cd in root and shoot tissues, Cd translocation factor (i.e. the shoot-to-root concentration ratio) and specific Cd uptake except that Cd treatment did not affect root Cd concentration at 5 µM Zn or Cd translocation factor at 100 µM Zn (Figure 3 and Table 1). Increasing solution Zn concentration decreased root Cd

concentration by 39-66%. The exception was that at 15 μM Cd, root Cd concentrations were similar when grown in solutions with 5 and 30 μM Zn (Figure 3a). Similarly, increasing solution Zn concentration from 5 to 30 μM did not influence shoot Cd concentration, but further increasing Zn concentration to 100 μM decreased the shoot tissue Cd concentration by 42-64% at both Cd levels (Figure 3b).

The effect of Zn addition on Cd translocation factor was concentration-dependent (Figure 3c). Increasing Zn from 5 to 30 μM in solutions did not affect the Cd translocation factor, while increasing solution Zn concentration from 5 to 100 μM increased Cd translocation by 69% at 5 μM Cd but decreased it by 29% at 15 μM Cd. Furthermore, increasing solution Zn concentration from 5 to 100 μM Zn did not alter specific Cd uptake, while it was 2-3 fold higher at 15 μM than at 5 μM Cd (Figure 3d).

Plant uptake and tissue Zn concentration

Increasing solution Zn addition generally increased root and shoot Zn concentrations except that increasing solution Zn from 30 to 100 μM Zn did not further increased plant Zn concentration at 15 μM Cd (Figure 4a, 4b and Table 1). However, the addition of Cd decreased root Zn concentration by > 50% at 100 μM Zn. In comparison, the effect of Cd addition on shoot Zn concentration was concentration-dependent (Figure 4b). The addition of 5 and 15 μM Cd decreased the shoot tissue Zn concentration by an average of 40% at 5 μM Zn, but did not affect it at 30 μM Zn, whereas 15 μM Cd decreased the shoot tissue Zn concentration by 50% at 100 μM Zn. As a result, the addition of 5 and 15 μM Cd increased the Zn translocation factor by 30-90%, except at 100 μM Zn where the addition of 15 μM Cd did not influence it (Figure 4c). In contrast, the addition of Cd only influenced specific Zn uptake at 100 μM Zn, with 38% (at 5 μM Cd) higher specific Zn uptake than the non-Cd treated plants (Figure 4d).

Zn speciation in plant samples using XAS

The XANES spectra for the eleven standard Zn compounds were examined (Figure 5). It was first noted that the spectra for the standard compounds in which Zn bound to a carboxyl group or was present as the free Zn^{2+} ion [i.e. $Zn(NO_3)_2$, oxalate, citrate, and polygalacturonate], were somewhat similar, with a white line peak at ca. 9,669.1-9,669.6 eV. Despite their overall similarity, subtle differences were observed in the magnitude of the white line peak or slight differences in the spectral features (Figure 6a). All seven of the other standard compounds showed distinctive features in their spectra. For example, the peak for cysteine was at 9,665.4 eV and was much flatter than others, while the peak for phosphate (9,667.0 eV) was also comparatively flat. The peak for phytate (9,666.7 eV) was broad, almost being double-peaked. Finally, the spectra of $[ZnCO_3]_2 \cdot [Zn(OH)_2]_3$ and $ZnCO_3 \cdot 2ZnO \cdot 3H_2O$ were somewhat similar with each other, but differed markedly from the spectrum of ZnO in the energy of their white line peak and their spectral features.

We then examined whether the freeze-drying process altered the XANES spectra of plant tissue samples. The spectra of freeze-dried and frozen hydrated shoots of *C. rossii* grown at 5 μM Zn were found to clearly differ from each other (Figure 6b). Specifically, differences between the spectra for the freeze-dried and hydrated tissues could be seen as: (i) a slight shift in the energy corresponding to the white line peak (9,668.3 versus 9,668.9 eV), and (ii) a lower but broader white line peak for the freeze-dried shoots than for the hydrated shoots (Figure 6b). Indeed, the LCF predicted that the Zn was present as Zn-oxalate (65-74%), and either Zn-histidine (35%) or Zn-cysteine (26%) in the frozen hydrated shoots. However, in the case of the freeze-dried shoots, 70% of the Zn was in the form of Zn-phytate, with 30% of Zn present as Zn-phosphate. It appeared that the freeze-drying process altered the speciation of Zn in plant tissues, and hence only hydrated tissues were examined hereafter.

We then compared the XANES spectra for all the root and shoot tissues. Overall, several important observations were noted. Firstly, all these spectra had a white line peak ca. 9,669.1 eV (Figure 7), with this energy value and the features of the spectra being somewhat visually similar to oxalate (Figures 5 and 6a). Secondly, the spectra for the various plant tissues appeared visually similar irrespective of the Zn and Cd concentration used, indicating the addition of Cd did not markedly alter the speciation of Zn within plant tissues (Figure 7). These observations were also confirmed by LCF, which predicted that the 48-87% of Zn in all root and shoot tissues was associated with oxalate after 10-d growth (Table 2). The remaining Zn in roots was bound to histidine, except for the plants grown in 5 μM Zn solutions with Cd addition, where the remaining Zn was either bound to histidine or cysteine. The increasing concentration of Zn or Cd in solution did not alter Zn speciation in the root tissues. However, the proportion of Zn-oxalate in shoots was 16% higher at 100 μM Zn than at 5 μM Zn, and the addition of Cd increased the Zn-oxalate by 11-20% at both 5 and 100 μM Zn.

Discussion

The effect of Zn and Cd on plant growth and root morphology

In the present study, Zn and Cd acted synergistically to inhibit the root growth of *C. rossii* (Figures 1 and 2). This observation is consistent with previous findings for other plant species that have been grown in either soils or solutions containing trace metals (Lu *et al.*, 2013a). In addition, the present study showed that the addition of Zn and Cd also changed root morphology – increasing solution concentrations of either Zn or Cd alone, or in combination, resulted in shorter and thicker roots (Figure 2). This impact had a greater effect on root morphological parameters (Figure 2) than on root weight (Figure 1a), particularly for root length. Similar effects have been reported in maize (*Zea mays*) and peanut (*Arachis hypogaea*) (Maksimović *et al.*, 2007, Lu *et al.*, 2013b).

The accumulation of Zn and Cd in plant tissues

High Zn supply reduced concentrations of Cd in root and shoot tissues of *C. rossii*, and high Cd likewise reduced tissue Zn concentrations. Thus these two heavy metals were antagonistic in their effects on tissue concentrations (Figures 3 and 4). Similar effects have been reported previously in other plant species (Hart *et al.*, 2002, Hart *et al.*, 2005, Jamali *et al.*, 2014).

This antagonistic effect of Zn and Cd on their tissue concentrations could be attributed to the decreased Zn and Cd accumulation in the plant, rather than to a 'dilution' effect. This is because the plants that grew in solutions with both Zn and Cd had similar shoot biomass, but significantly smaller root biomass compared with the plants grown in solutions with the corresponding concentrations of Zn or Cd alone. There are several possible reasons to explain this decreased Zn and Cd accumulation. Firstly, the total capacity of root uptake was reduced by the addition of Zn and Cd. Generally, plant root parameters determine the capacity of plants to acquire water and nutrients, and the metal uptake capacity is strongly related to the total root surface area and specific root uptake capacity per unit root surface area (Li et al., 2009, Guerrero-Campo *et al.*, 2006, Tachibana and Ohta, 1983). In the present study, the addition of Cd or Zn in solution decreased the root surface area by up to 65% with high concentrations of Zn and Cd together, compared to the treatments with Zn or Cd alone (Figure 2b), although the specific uptake capacity of Zn or Cd was similar or even higher (Figures 3d and 4d).

A second reason for the antagonistic behavior of Cd and Zn is the decreased activity of Zn^{2+} and Cd^{2+} at the plasma membrane surface caused by high concentrations of the other metal ion, despite the speciation of Zn and Cd in the nutrient solutions not being altered. It has been reported that increasing the concentrations of cations reduces the negativity of the electrical potential at the surface of plasma membrane, with this then decreasing the activities of metal cations at the membrane surface (Kopittke *et al.*, 2011a, Wang *et al.*, 2011). Ion activities at the plasma membrane surface were calculated as described by Kopittke *et al.* (2014), and it was found that for

a given Zn level, the addition of Cd only decreased the negativity of the electrical potential slightly, with only small changes in the activity of Zn^{2+} at the plasma membrane surface (Table 3). Furthermore, increasing solution Zn concentrations from 5 to 30 or 100 μM markedly reduced the negativity of the electrical potential, resulting in predicted decreases in the activities of Cd^{2+} at the plasma membrane surface of 13% (30 μM) and 36.5% (100 μM) (Table 3). Thus, the decreased accumulation of Cd in plant tissues caused by increasing Zn (Figure 3) is likely related (at least in part) to a decreased activity of Cd^{2+} at the surface of outer plasma membrane. In contrast, the decreased Zn accumulation in plants caused by elevated concentrations of Cd could not explain by changes in the activity of Zn^{2+} at the plasma membrane surface.

A third possible reason for the antagonistic inhibition of Zn and Cd accumulation might be attributed to the competition between the two metals for transporters at the root cell plasma membrane. As a non-essential element, Cd^{2+} is likely to enter plant cells through divalent cation carriers or channels of low specificity, especially for Zn^{2+} given the similar properties of the two metal ions (Verkleij *et al.*, 2009, Clemens, 2006). This competition between Cd and Zn for root uptake is consistent with that observed in Cd/Zn hyperaccumulator *Noccaea (Thlaspi) caerulescens*, although a high-affinity Cd transporter is involved in Cd uptake in the Ganges ecotype of *N. caerulescens* (Lombi *et al.*, 2001). Similar result was also reported in the roots of bread wheat *(Triticum aestivum)* and durum wheat *(T. turgidum)*, where Zn and Cd appeared to be transported via a common carrier whilst the affinity of the transporter was greater for Cd than for Zn (Hart *et al.*, 2002).

Although the addition of Cd decreased Zn concentration in both the root and shoot tissues, the magnitude of the decrease was substantially higher in the roots, thereby indicating that Cd decreased Zn uptake but enhanced its translocation from root to shoot in *C. rossii* (Figure 4). This observation that Cd addition increases Zn translocation is consistent with that observed in *S. alfredii* (Li *et al*., 2009), but differs from that reported in *Thlaspi caerulescens* (*Noccaea caerulescens*) and *P. griffithii* (*Qiu et al*., 2011) where Cd addition significantly decreased Zn translocation. This enhanced Zn translocation in the present study could not be explained by changes in the speciation of Zn within plant tissues given that the addition of Cd did not alter Zn speciation in the plant root tissues (Figure 7 and Table 2). One possibility for this Cd-induced increase in Zn translocation is that the Cd decreased vacuolar Zn sequestration in plant roots by competing for the cation/H^+ antiporter to move across the tonoplast and/or changing the electrochemical potential difference for H^+, which energizes the pumping of Zn^{2+} and Cd^{2+} into the vacuole (Clemens, 2006, Verkleij *et al*., 2009). Another possible mechanism is that in the presence of Cd, more Zn was required by the plant shoots to maintain the plant growth with the high Cd concentrations in the shoot tissue, given the important role of Zn in many biological systems, including enzyme reactions, gene expression and protein production (Marschner, 2011). It has been reported that Cd and Zn induced differential molecular responses in plants, and a number of proteins participated in the inhibition of Cd uptake and Cd detoxification with the supply of Zn (Wang et al., 2016). However, further research is required to test these hypotheses.

The effect of Zn on the translocation of Cd was smaller and concentration-dependent, with 100 μM Zn enhancing Cd translocation at 5 μM Cd but decreasing it at 15 μM Cd (Figure 3c). Increased Cd translocation by Zn addition had also been reported in *P. griffithii* (Qiu *et al*., 2011), which may also be due to the competition for sequestration in vacuoles and/or the elevated expression of the Cd transporter at low Cd level (Clemens, 2006; Verkleij *et al*., 2009; Verret *et al.* 2004). However, the decreased Cd translocation observed in the present study for the treatment containing 100 μM Zn and 15 μM Cd might be due to the competitive transport at high Cd levels, but this still needs further study.

In the present study, interestingly, the effects of Cd addition on Zn uptake and translocation were greater than the effects of Zn on Cd, even when the level of Zn in solutions was 20 times higher than the Cd level. Only the highest level of Zn (100 μM) significantly decreased the uptake and influenced the translocation of Cd in *C. rossii,* confirming *C. rossii* is a promising candidate for phytoextraction of Cd in contaminated soils coexisting with high levels of Zn (Zhang *et al*., 2014).

Speciation of Zn in plant tissues

In the present study, LCF predicted that Zn was predominantly (48-87%) bound to oxalate in the root tissues of *C. rossii* (Figure 7 and Table 2). This is consistent with previous studies showing that the organic acids play important role in chelating Zn in plant tissues (Küpper *et al.*, 2004, Küpper *et al.*, 1999). However, most previous studies have reported that malate or citrate, rather than oxalate, are the most important organic anions for the complexation of Zn in plant tissues. For example, Sarret *et al.* (2002) found that more than 67% of Zn in the aerial tissues of *A. halleri* was octahedrally coordinated and complexed to malate. In addition, Lu *et al.* (2014) reported that 41-67% of Zn in the shoots of *S. alfredii* was complexed with malate, while Zn-citrate and Zn-cell wall complexes dominated in the roots. The authors attributed the complexation of Zn-malate partially to malate having the highest concentrations among the measured organic acids in the tissues of *S. alfredii*. In contrast, oxalate was the most abundant organic acid among seven organic acids in the roots of *C. rossii*, while malate was the organic acid with the highest concentration in the shoots (Cheng *et al*., 2018). Indeed, Zn has a stronger affinity for oxalate (stability constants log K 1.7-6.4) than for malate (stability constants log K 1.7-2.9) (Martell and Smith, 1974), and so it is not unexpected that Zn-oxalate complexes formed when high concentrations of oxalate occur in the tissue. It should also be noted that complexes of Zn-oxalate were also found in the shoots of *T. caerulescens* (Salt *et al.*, 1999) and the roots of tobacco (*Nicotiana tabacum*) (Straczek *et al.*, 2008), although the proportion was smaller (0-30%) than in the tissues of *C. rossii*. Therefore, Zn-oxalate appeared to play an important role in *C. rossii*'s tolerance to high Zn concentrations in its tissue. However, the speciation of Zn with the roots was not greatly affected by the addition of Cd or increasing Zn concentration in solution, indicating that the enhanced Zn translocation in plants upon the addition of Cd was not due to the changes of Zn speciation within plant roots.

It was found that Zn-oxalate was also the dominant Zn species (50-87%) in the shoots of *C. rossii,* with the remaining 13-50% of Zn present as Zn-histidine (Figure 7 and Table 2), which was similar to the Zn speciation reported for the shoots of *T. caerulescens* (Küpper *et al*., 2004). In addition, the observation that the proportion of Zn-histidine in the shoot tissues decreased with the addition of Cd is in agreement with Küpper *et al*. (2004), who found the proportion of Zn-histidine in the mature leaf of *T. caerulescens* decreased from 40 to 1% upon the addition of 100 μM Cd to nutrient solutions containing 10 μM Zn. Furthermore, in the present study, we found that the proportion of Zn-oxalate in the shoots increased from 50 to 87% with the addition of Cd and increasing Zn in the solution (Table 2). This indicates that the sequestration of Zn in vacuoles with oxalate may be an important strategy in the aerial parts of *C. rossii* to detoxify the accumulated Zn when the plant is grown with high metal stress.

The present study used hydrated (frozen) tissue samples for the XANES analyses as we found differences between the spectra of the hydrated and freeze-dried samples (Figure 6b). There have long been concerns that the freeze-drying process could produce experimental artifacts (Sarret *et al*., 2002, Küpper *et al*., 2004, Sarret *et al.*, 2009). For example, using freeze-dried samples, it was reported that Zn was associated solely with phosphate in leaves of *A. lyrata* (Sarret *et al*., 2002), while for hydrated (frozen) leaves 75% of Zn was either free Zn^{2+} or was complexed with carboxyl groups, with the remaining 25% of the Zn being as Zn phosphate (Sarret *et al*., 2009). The present study has provided further evidence that freeze-drying changed the Zn speciation in plant tissues. Using predictions from LCF, we found that Zn was predominately complexed to oxalate and histidine in the frozen hydrated shoots, but as Zn phytate and Zn phosphate in the freeze-dried

samples. This indicates that dehydration resulted in Zn-phosphate and Zn-phytate precipitates forming from the Zn originally present in aqueous state, because the Zn stored in the vacuole may enter the cytoplasm and chloroplasts during freeze drying (Küpper *et al*., 2004, Küpper *et al*., 1999). However, these artifacts for Zn speciation caused by freeze-drying differ from that observed for Cd, where freeze drying has been found previously not to alter speciation (Cheng *et al*., 2016, Isaure *et al.*, 2006). Therefore, the potential impact of the sample preparation process should be considered when performing analyses to investigate the speciation of Zn in plant tissues.

In conclusion, the presence of both Zn and Cd within the nutrient solution resulted in a negative effect on root growth of *C. rossii*, but an antagonistic pattern in their accumulation in shoots. Furthermore, the addition of Cd to the nutrient solution significantly enhanced the translocation of Zn from roots to shoots, while only the highest level of Zn (100 μM) influenced the translocation of Cd in *C. rossii*, with increasing Cd translocation at 5 μM Cd but decreasing it at 15 μM Cd. However, this enhanced Zn translocation in plants upon the addition of Cd did not result from the changes of Zn speciation within plant tissues. Rather, in both the roots and shoots, Zn was predominantly bound to oxalate (48-87%), with the remaining Cd present as Zn-hisitidine or Zn-cysteine. The present study showed the competition between Cd and Zn uptake and accumulation in *C. rossii*, which needs to be considered should *C. rossii* be used to phytoremediate Cd/Zn contaminated soils.

Acknowledgements

This research was undertaken on the XAS beamline (Project AS171/XAS/11713) at the Australian Synchrotron, part of the Australian Nuclear Science and Technology organization (ANSTO). We thank Drs. Peter Kappen and Chris Glover (Australian Synchrotron) for their advice on use of XAS, Mr. James O'Sullivan (La Trobe University, Australia) for helping with the XAS analyses at the Australian Synchrotron. Funding from the Australian Research Council for a Linkage Project for C.T. (LP100100800) and a Future Fellowship for P.M.K. (FT120100277) is also acknowledged.

References

Benáková M, Ahmadi H, Dučaiová Z, Tylová E, Clemens S, Tůma J (2017) Effects of Cd and Zn on physiological and anatomical properties of hydroponically grown *Brassica napus* plants. Environ Sci Pollut Res 24: 20705-20716

Cheng MM, Wang P, Kopittke PM, Wang A, Sale PWG, Tang C (2016) Cadmium accumulation is enhanced by ammonium compared to nitrate in two hyperaccumulators, without affecting speciation. J Exp Bot 67: 5041-5050

Cheng MM, Wang A, Liu Z**,** Gendall AR, Rochfort S, Tang C (2018) Sodium chloride decreases cadmium accumulation and changes the response of metabolites to cadmium stress in the halophyte *Carpobrotus rossii*. Ann Bot https://doi.org/10.1093/aob/mcy077

Clemens S (2006) Toxic metal accumulation, responses to exposure and mechanisms of tolerance in plants. Biochimie 88: 1707-1719

Cojocaru P, Gusiatin ZM, Cretescu I (2016) Phytoextraction of Cd and Zn as single or mixed pollutants from soil by rape (*Brassica napus*). Environ Sci Pollut Res 23: 10693-10701

Guerrero-Campo J, Palacio S, Perez-Rontome C, Montserrat-Marti G (2006) Effect of root system morphology on root-sprouting and shoot-rooting abilities in 123 plant species from eroded lands in north-east Spain. Ann Bot 98: 439-447

Hart JJ, Welch RM, Norvell WA, Clarke JM, Kochian LV (2005) Zinc effects on cadmium accumulation and partitioning in near-isogenic lines of durum wheat that differ in grain cadmium concentration. New Phytol 167: 391-401

Hart JJ, Welch RM, Norvell WA, Kochian LV (2002) Transport interactions between cadmium and zinc in roots of bread and durum wheat seedlings. Physiol Plant 116: 73-78

Hunt R (2012) Basic growth analysis: plant growth analysis for beginners. Springer Science and Business Media

Isaure MP, Fayard B, Saffet G, Pairis S, Bourguignon J (2006) Localization and chemical forms of cadmium in plant samples by combining analytical electron microscopy and X-ray spectromicroscopy. Spectrochim Acta B 61: 1242-1252

Jamali N, Ghaderian SM, Karimi N (2014) Effects of cadmium and zinc on growth and metal accumulation of *Mathiola flavida* boiss. Envir Eng Manag J 13: 2937-2944

Kopittke PM, Blamey FPC, Kinraide TB, Wang P, Reichman SM, Menzies NW (2011a) Separating multiple, short-term, deleterious effects of saline solutions on the growth of cowpea seedlings. New Phytol 189: 1110-1121
Kopittke PM, Menzies NW, de Jonge MD, McKenna BA, Donner E, Webb RI, Paterson DJ, Howard DL, Ryan CG, Glover CJ, Scheckel KG, Lombi E (2011b) In situ distribution and speciation of toxic copper, nickel, and zinc in hydrated roots of cowpea. Plant Physiol 156: 663-673
Kopittke PM, Wang P, Menzies NW, Naidu R, Kinraide TB (2014) A web-accessible computer program for calculating electrical potentials and ion activities at cell-membrane surfaces. Plant Soil 375: 35-46
Küpper H, Mijovilovich A, Meyer-Klaucke W, Kroneck PMH (2004) Tissue- and age-dependent differences in the complexation of cadmium and zinc in the cadmium/zinc hyperaccumulator *Thlaspi caerulescens* (Ganges ecotype) revealed by X-ray absorption spectroscopy. Plant Physiol 134: 748-757
Küpper H, Zhao FJ, McGrath SP (1999) Cellular compartmentation of zinc in leaves of the hyperaccumulator *Thlaspi caerulescens*. Plant Physiol 119: 305-311
Li TQ, Yang XE, Lu LL, Islam E, He ZL (2009) Effects of zinc and cadmium interactions on root morphology and metal translocation in a hyperaccumulating species under hydroponic conditions. J Hazard Mater 169: 734-741
Lombi E, Zhao FJ, McGrath SP, Young SD, Sacchi GA (2001) Physiological evidence for a high-affinity cadmium transporter highly expressed in a *Thlaspi caerulescens* ecotype. New Phytol 149: 53-60
Lu LL, Liao XC, Labavitch J, Yang X, Nelson E, Du YH, Brown PH, Tian SK (2014) Speciation and localization of Zn in the hyperaccumulator *Sedum alfredii* by extended X-ray absorption fine structure and micro-X-ray fluorescence. Plant Physiol Bioch 84: 224-232
Lu LL, Tian SK, Yang XE, Peng HY, Li TQ (2013a) Improved cadmium uptake and accumulation in the hyperaccumulator *Sedum alfredii*: the impact of citric acid and tartaric acid. J Zhejiang Univ-Sc B 14: 106-114
Lu Z, Zhang Z, Su Y, Liu C, Shi G (2013b) Cultivar variation in morphological response of peanut roots to cadmium stress and its relation to cadmium accumulation. Ecotox Environ Safe 91: 147-155
Mahar A, Wang P, Ali A, Awasthi MK, Lahori AH, Wang Q, Li RH, Zhang ZQ (2016) Challenges and opportunities in the phytoremediation of heavy metals contaminated soils: A review. Ecotox Environ Safe 126: 111-121
Maksimović I, Kastori R, Krstić L, Luković J (2007) Steady presence of cadmium and nickel affects root anatomy, accumulation and distribution of essential ions in maize seedlings. Biol Plantarum 51: 589-592
Marschner P (2011) Marschner's mineral nutrition of higher plants. Academic Press
Martell AE, Smith RM (1974) Critical stability constants. Plenum Press, New York
Monsant AC, Kappen P, Wang Y, Pigram PJ, Baker AJ, Tang C (2011) In vivo speciation of zinc in *Noccaea caerulescens* in response to nitrogen form and zinc exposure. Plant Soil 348: 167-183
Nicholson FA, Jones KC, Johnston AE (1994) Effect of phosphate fertilizers and atmospheric deposition on long-term changes in the cadmium content of soils and crops. Environ Sci Technol 28: 2170-2175
Qiu RL, Thangavel P, Hu PJ, Senthilkumar P, Ying RR, Tang YT (2011) Interaction of cadmium and zinc on accumulation and sub-cellular distribution in leaves of hyperaccumulator *Potentilla griffithii*. J Hazard Mater 186: 1425-1430
Ravel B, Newville M (2005) ATHENA, ARTEMIS, HEPHAESTUS: data analysis for X-ray absorption spectroscopy using IFEFFIT. J Synchrotron Radiat 12: 537-541
Salt DE, Prince RC, Baker AJ, Raskin I, Pickering IJ (1999) Zinc ligands in the metal hyperaccumulator *Thlaspi caerulescens* as determined using X-ray absorption spectroscopy. Environ Sci Technol 33: 713-717
Sarret G, Saumitou-Laprade P, Bert V, Proux O, Hazemann JL, Traverse AS, Marcus MA, Manceau A (2002) Forms of zinc accumulated in the hyperaccumulator *Arabidopsis halleri*. Plant Physiol 130: 1815-1826. doi: 10.1104/pp.007799
Sarret G, Willems G, Isaure MP, Marcus MA, Fakra SC, Frerot H, Pairis S, Geoffroy N, Manceau A, Saumitou-Laprade P (2009) Zinc distribution and speciation in *Arabidopsis halleri* × *Arabidopsis lyrata* progenies presenting various zinc accumulation capacities. New Phytol 184: 581-595
Straczek A, Sarret G, Manceau A, Hinsinger P, Geoffroy N, Jaillard B (2008) Zinc distribution and speciation in roots of various genotypes of tobacco exposed to Zn. Environ Exp Bot 63: 80-90
Tachibana Y, Ohta Y (1983) Root surface area, as a parameter in relation to water and nutrient uptake by cucumber plant. Soil Sci Plant Nutr 29: 387–392
Verkleij JAC, Golan-Goldhirsh A, Antosiewisz DM, Schwitzguebel JP, Schroder P (2009) Dualities in plant tolerance to pollutants and their uptake and translocation to the upper plant parts. Environ Exp Bot 67: 10-22
Verret F, Gravot A, Auroy P, Leonhardt N, David P, Nussaume L, Vavasseur A, Richaud P (2004) Overexpression of AtHMA4 enhances root-to-shoot translocation of zinc and cadmium and plant metal tolerance. FEBS Letters 576: 306-312
Wang P, Kinraide TB, Zhou DM, Kopittke PM, Peijnenburg WJGM (2011) Plasma membrane surface potential: dual effects upon ion uptake and toxicity. Plant Physiol 155: 808-820
Wang Y, Wang X, Wang C, Wang R, Peng F, Xiao X, Zeng J, Fan X, Kang H, Sha L (2016) Proteomic profiling of the interactions of Cd/Zn in the roots of dwarf polish wheat (*Triticum polonicum* L.). Fronts Plant Sci 7: 1378.
Zhang CJ, Sale PWG, Doronila AI, Clark GJ, Livesay C, Tang CX (2014) Australian native plant species *Carpobrotus rossii* (Haw.) Schwantes shows the potential of cadmium phytoremediation. Environ Sci Pollut Res 21: 9843-9851.

Table 1. Significant levels of Cd and Zn treatment effects and their interactions on plant growth and metal concentration in *Carpobrotus rossii* grown for 10 d in solutions with various concentrations of Cd (0, 5 and 15 μM) and Zn (5, 30 and 100 μM)**.**

Measurements	**Zn**	**Cd**	**Zn × Cd**
Root weight	***	**	**
Shoot weight	*	n.s.	*
RGR	***	*	***
Root length	***	***	***
Root surface	***	***	*
Root diameter	***	***	n.s.
Root Zn concentration	***	***	*
Shoot Zn concentration	***	***	***
Zn translocation factor	*	***	*
Specific Zn uptake	***	n.s.	**
Root Cd concentration	***	***	*
Shoot Cd concentration	***	***	***
Cd translocation factor	n.s.	***	**
Specific Cd uptake	n.s.	***	n.s.

n.s., *, **, *** indicate $P>0.05$, $P<0.05$, $P<0.01$, $P<0.001$, respectively.

The two-way analysis for plant root weight, root length, root surface, Zn/Cd concentration in tissues, Zn translocation factor and specific Zn/Cd uptake were performed after square-root transformation.

Table 2. The predicted speciation of Zn in root and shoot tissues of *Carpobrotus rossii* grown for 10 d in solutions with different concentrations of Cd (0, 5 and 15 μM) and Zn (5 and 100 μM) as calculated using linear combination fitting (LCF) of the K-edge XANES spectra.

Treatment		R-factor	Zn-oxalate	Zn-histidine	Zn-cysteine	R-factor	Zn-oxalate	Zn-histidine
Zn (μM)	Cd (μM)	**Root**				**Shoot**		
5	0	0.00082	65.1 (1.1)	34.9 (5.3)		0.00079	49.9 (4.3)	50.1 (1.2)
5	5	0.00083	73.5 (0.6)		26.5 (0.6)	0.00170	69.7 (1.6)	30.3 (4.0)
		0.00106	49.5 (1.2)	50.5 (1.2)				
5	15	0.00292	76.8 (4.0)		23.2 (1.1)	0.00129	61.9 (1.3)	38.1 (1.6)
		0.00408	59.4 (4.6)	40.6 (2.5)				
100	0	0.00052	52.7 (0.8)	47.3 (0.8)		0.00362	66.0 (3.3)	34.0 (2.2)
100	15	0.00069	47.5 (1.0)	52.5 (6.6)		0.00180	86.9 (1.7)	13.1 (5.3)

The values in brackets show the percentage variation in the calculated values. The goodness of fit is indicated by the R-factor. R factor = Σ_i (experiment – fit)^2 / Σ_i (experimental)^2, where the sums are over the data points in the fitting region.

Table 3. The calculated cell membrane surface potentials (Ψ_0^o), and Cd^{2+} and Zn^{2+} activities in the bulk-phase medium ($\{Cd^{2+}\}_b$ and $\{Zn^{2+}\}_b$), and at the cell membrane surface ($\{Cd^{2+}\}_0^o$ and $\{Zn^{2+}\}_0^o$) in the different treatments.

Treatment		Ψ_0^o	$\{Zn^{2+}\}_b$	$\{Zn^{2+}\}_0^o$	$\{Cd^{2+}\}_b$	$\{Cd^{2+}\}_0^o$
Zn (μM)	Cd (μM)	(mV)	(μM)	(μM)	(μM)	(μM)
	0	-39.5	3.8	81.9	-	-
5	5	-39.2	3.8	80.1	3.5	73.6
	15	-38.7	3.8	76.7	10.4	211.6
	0	-37.7	22.6	424.0	-	-
30	5	-37.4	22.6	416.1	3.5	63.6
	15	-37.0	22.6	401.0	10.4	183.8
	0	-33.6	75.0	1027.5	-	-
100	5	-33.5	75.0	1013.8	3.4	46.1
	15	-33.1	74.9	987.5	10.2	134.8

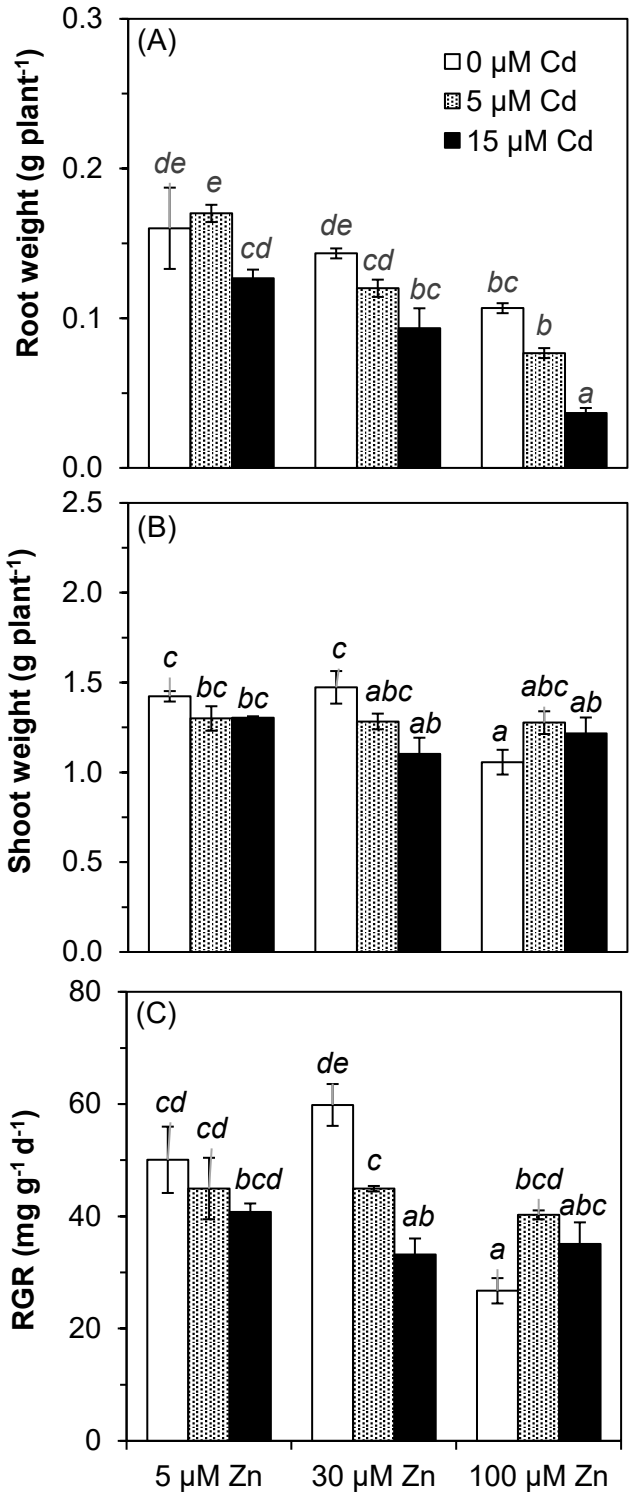

Figure 1. Dry weights of roots (A), shoots (B), and relative growth rate (RGR) of the entire plant (C) of *Carpobrotus rossii* grown for 10 d in solutions with different concentrations of Cd (0, 5 and 15 µM) and Zn (5, 30 and 100 µM). Error bars represent ± SEM of three replicates. Means with a common letter did not differ significantly (Duncan's test, $P< 0.05$). The two-way analysis for plant root weight was performed after square-root transformation

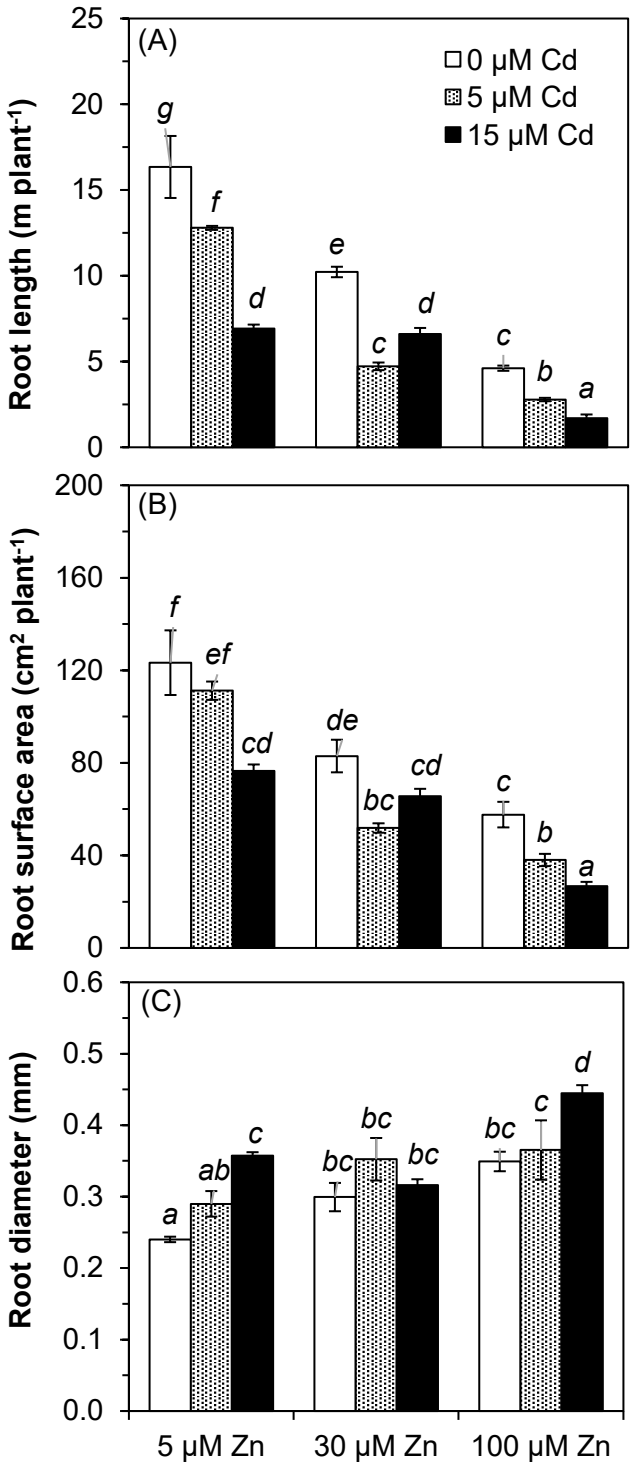

Figure 2. Root length (A), root surface area (B), and root diameter (C) of *Carpobrotus rossii* grown for 10 d in solutions with different concentrations of Cd (0, 5 and 15 µM) and Zn (5, 30 and 100 µM). Error bars represent ± SEM of three replicates. Means with a common letter did not differ significantly (Duncan's test, $P < 0.05$). The two-way analysis for root length and root surface was performed after square-root transformation.

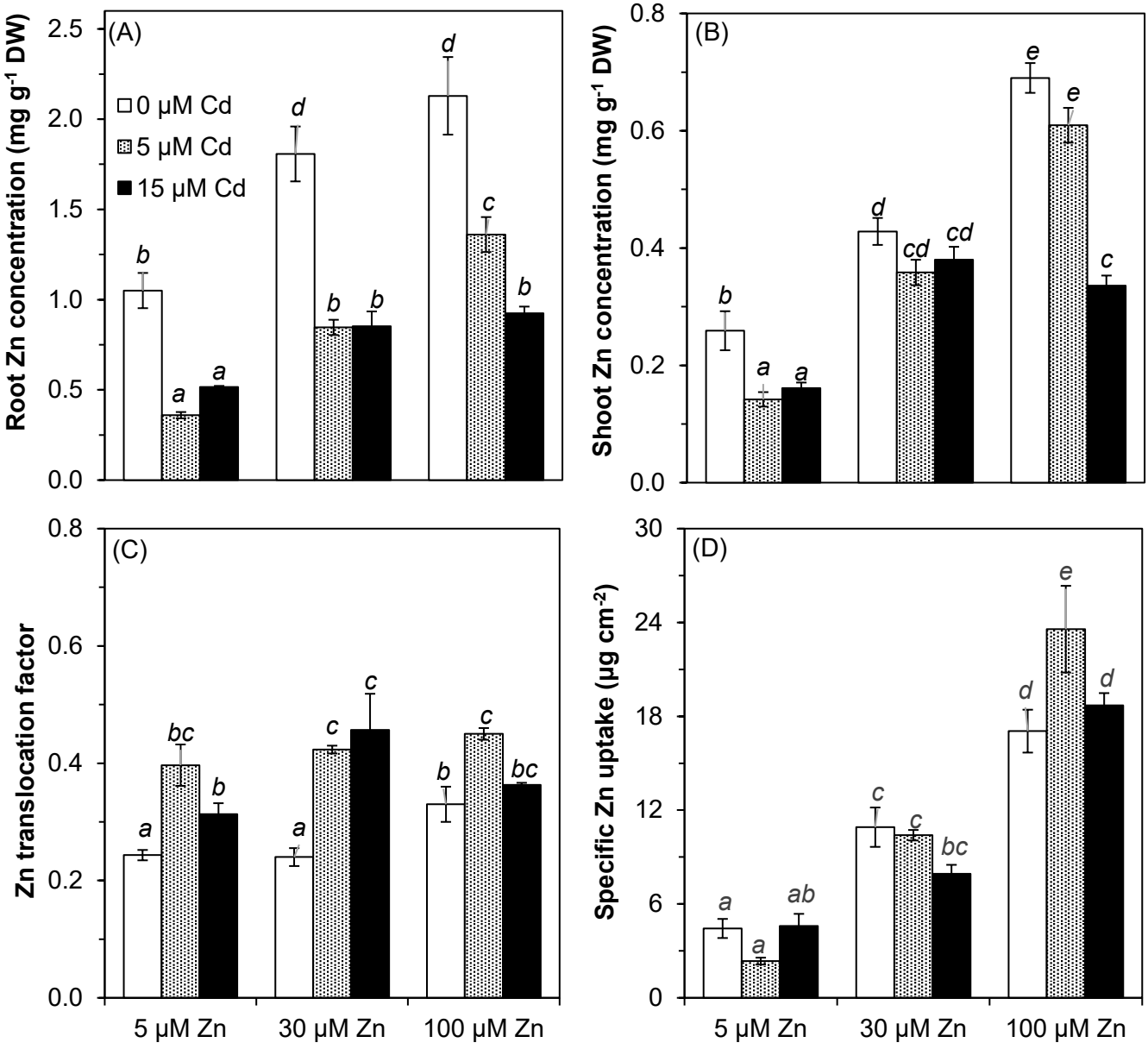

Figure 3. The concentration of Zn in root (A) and shoot tissues (B) of *Carpobrotus rossii*. The Zn translocation factor (shoot-to-root Zn concentration ratio) (C) and specific Zn uptake (D) are also given. Plants were grown for 10 d in solutions with different concentrations of Cd (0, 5 and 15 µM) and Zn (5, 30 and 100 µM). Error bars represent ± SEM of three replicates. Means with the same letter did not differ significantly (Duncan's test, $P < 0.05$). The two-way analysis for Cd concentration in roots and shoots, and specific Cd uptake was performed after square-root transformation

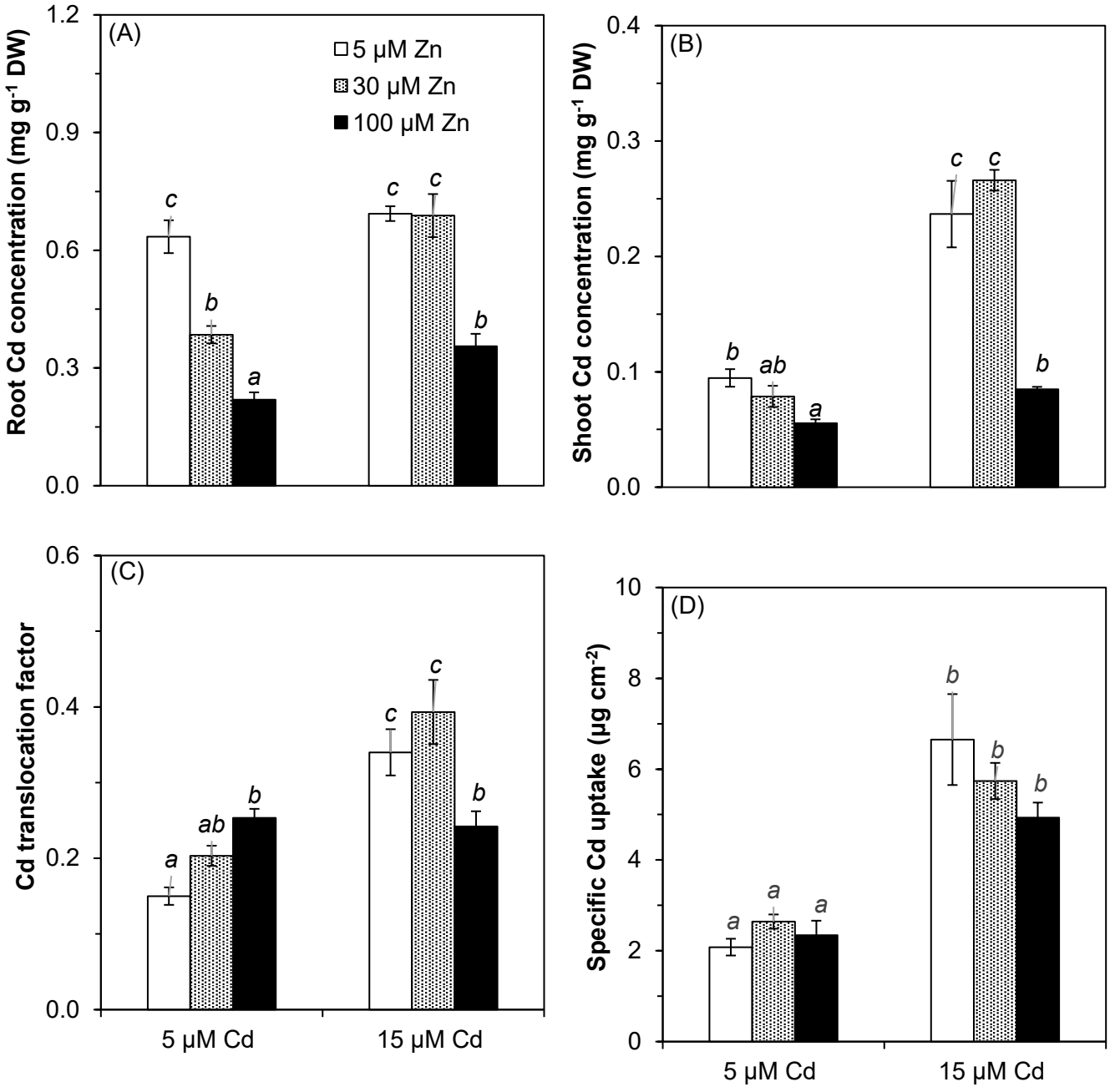

Figure 4. The concentration of Cd in root (A) and shoot tissues (B) of *Carpobrotus rossii*. The Cd translocation factor (shoot-to-root Cd concentration ratio) (C) and specific Cd uptake (D) are also given. Plants were grown for 10 d in solutions with different concentrations of Cd (0, 5 and 15 µM) and Zn (5, 30 and 100 µM). Error bars represent ± SEM of three replicates. Means with a common letter did not differ significantly (Duncan's test, $P < 0.05$). The two-way analysis was performed after square-root transformation.

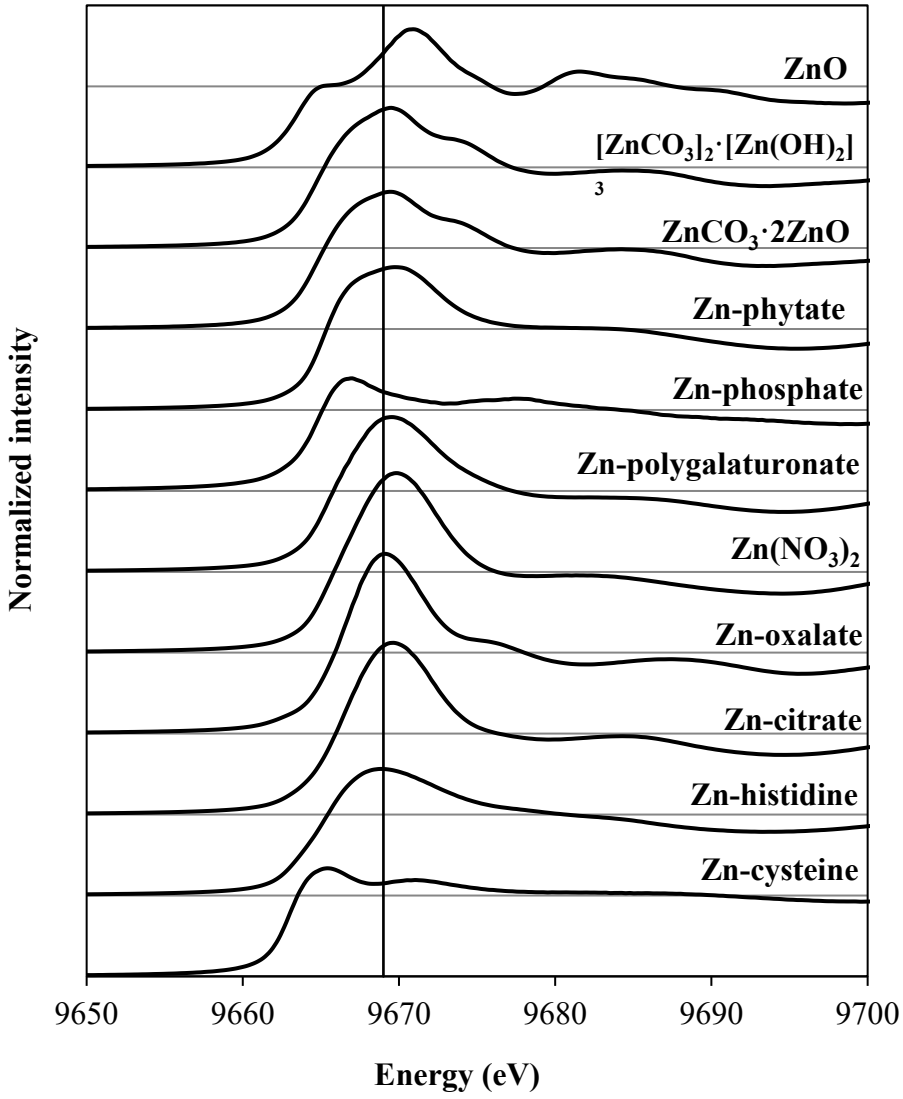

Figure 5. Normalized K-edge XANES spectra of the Zn standards. The vertical black line represents the white-line peak of Zn-oxalate (9,669.1 eV).

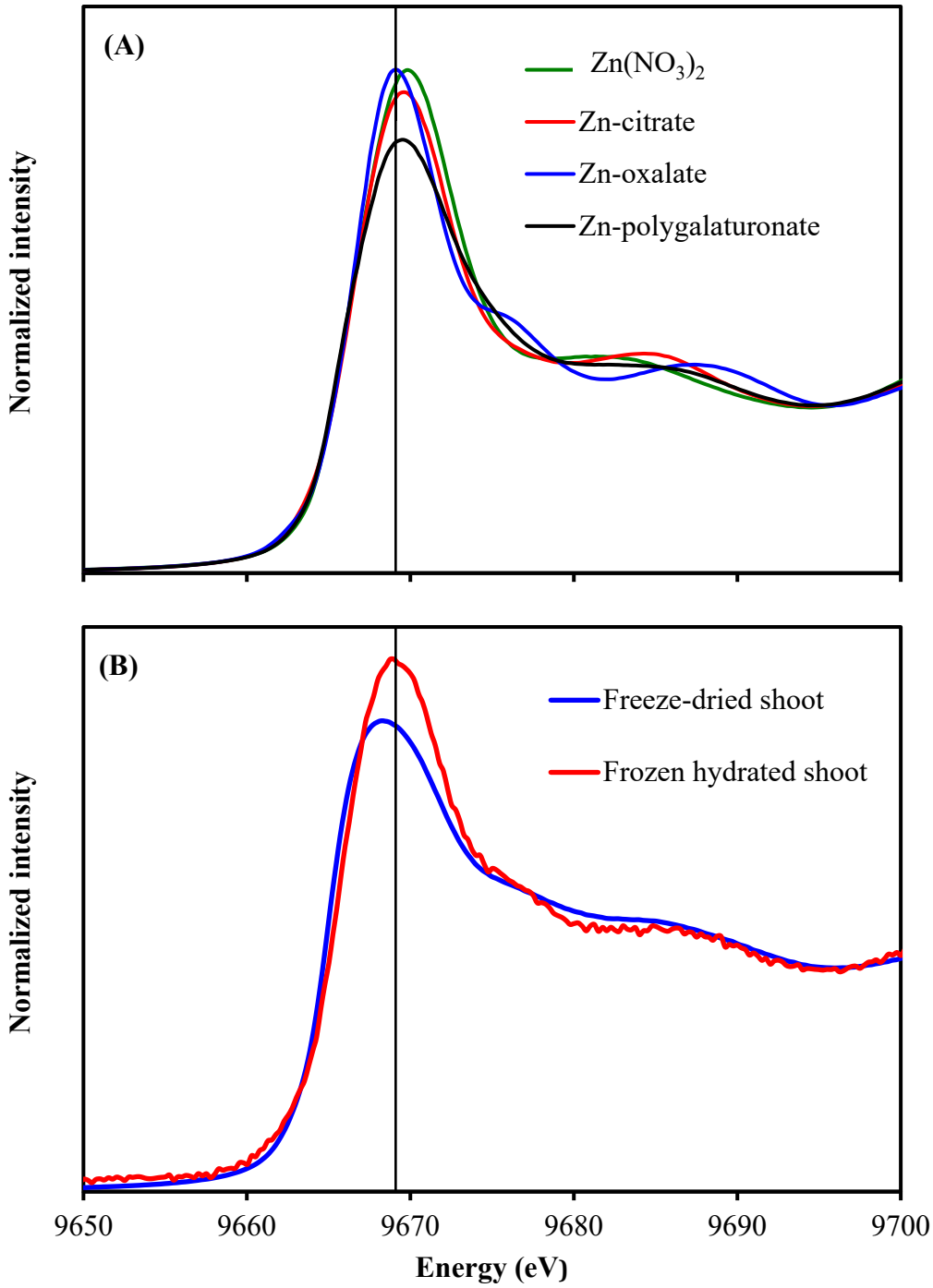

Figure 6. Normalized Zn K-edge XANES spectra comparing four standards of $Zn(NO_3)_2$, Zn-oxalate, Zn-citrate, and Zn-polygalacturonate (A) and spectra comparing freeze-dried shoots and frozen hydrated shoots of *Carpobrotus rossii* grown for 10 d in solutions with 5 µM Zn (B). The vertical black line represents the white-line peak of Zn-oxalate (9,669.1 eV).

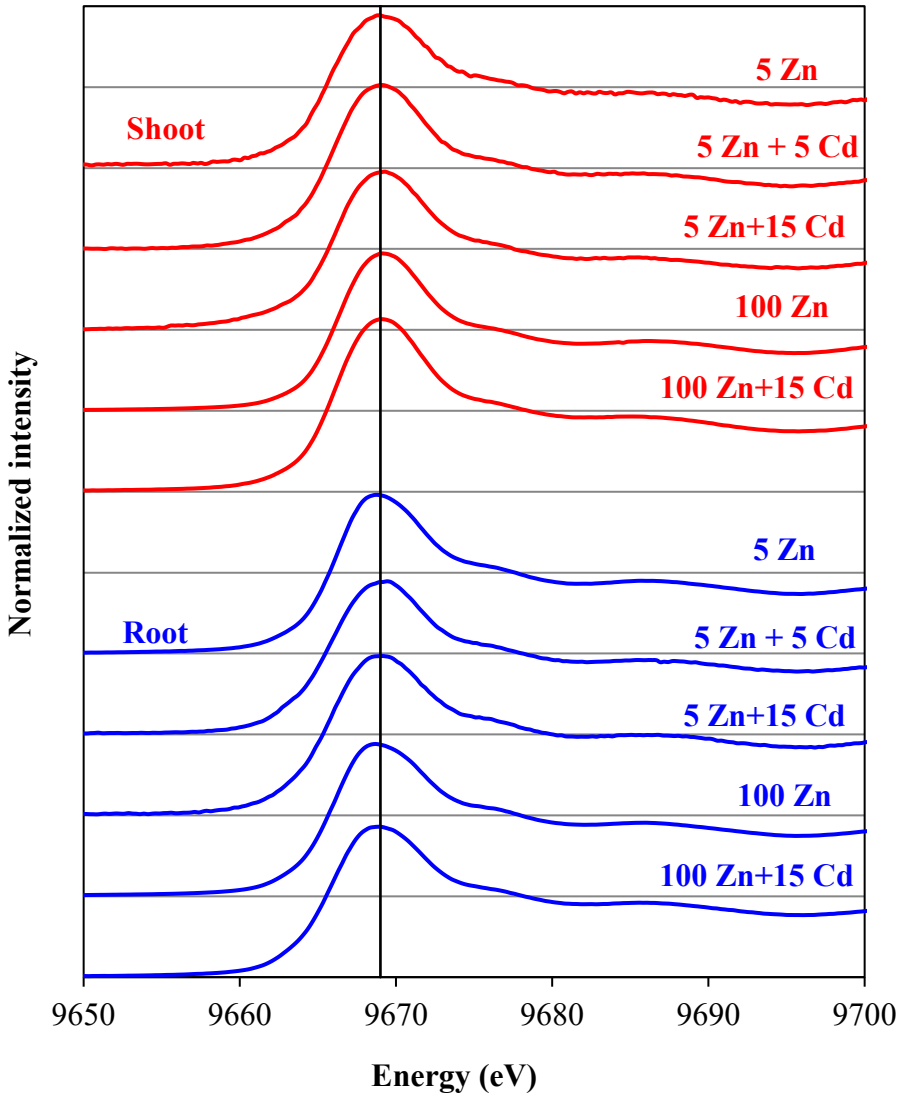

Figure 7. Normalized Zn K-edge XANES spectra for the frozen hydrated shoot and root tissues of *Carpobrotus rossii* grown for 10 d in solutions with different concentrations of Cd (0, 5 and 15 μM) and Zn (5 and 100 μM). The vertical black line represents the white-line peak of Zn-oxalate (9,669.1 eV).